

7  
4  
9

V393  
.R46

09

MASS. INST. OF TECHNOLOGY  
Department of Naval Architecture

MIT LIBRARIES



3 9080 02754 1058

# NAVY DEPARTMENT

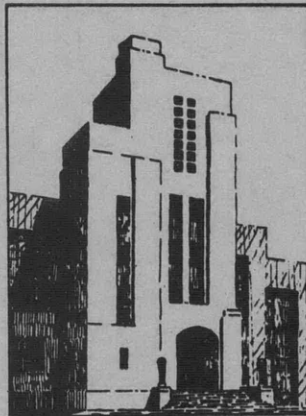
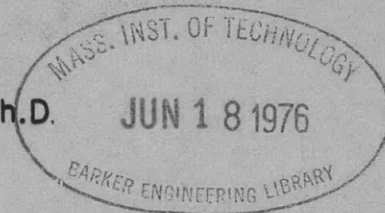
THE DAVID W. TAYLOR MODEL BASIN

WASHINGTON 7, D.C.

## THE RESPONSE OF SIMPLE FLOATING TARGETS TO UNDERBOTTOM EXPLOSION ATTACK

by

Erich Buchmann, Ph.D.

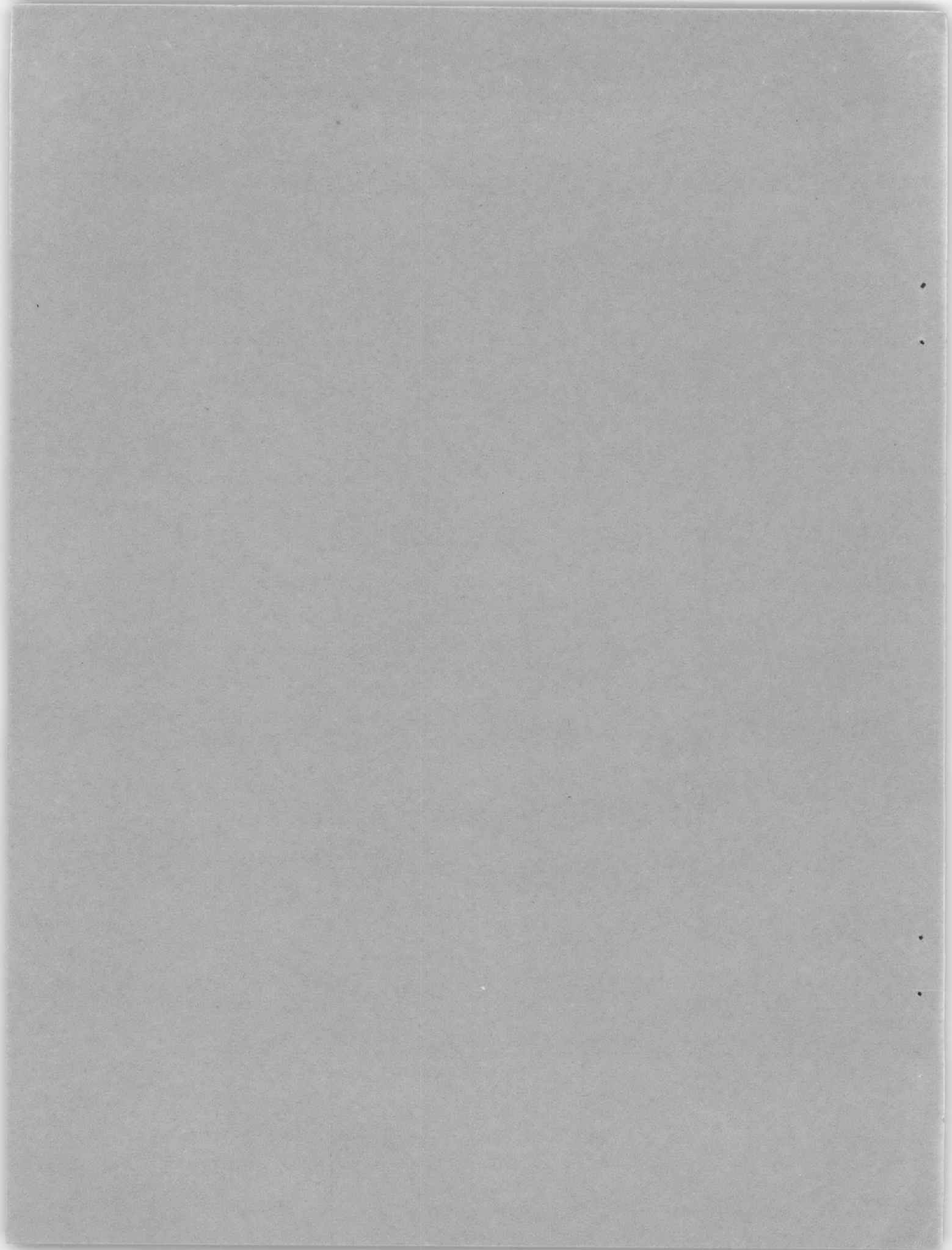


June 1951

Report 749

NS 724-002

JUL 12 1951



INITIAL DISTRIBUTION

Copies

15 Chief, Bureau of Ships, Project Records (Code 324)

3 Chief, Bureau of Ordnance

2 Chief of Naval Research

1 Director, Naval Research Laboratory, Washington 20, D.C.  
Attn: Mr. Hartbower, Code 3550

3 Commanding Officer, Naval Training School, Massachusetts Institute  
of Technology, Cambridge 39, Mass.

3 Commander, Naval Ordnance Laboratory, Silver Spring, Md.

3 Commander, Norfolk Naval Shipyard, Underwater Explosions Research  
Unit (Code 205), Portsmouth, Va.

1 Chief, Armed Forces Special Weapons Project, the Pentagon,  
Washington, D.C.

1 INSMAT, New York Naval Shipyard for:  
Captain N.W. Gokey, USN (Ret.), Webb Institute

1 Commander, Boston Naval Shipyard, Boston 29, Mass.

1 Commander, Puget Sound Naval Shipyard, Bremerton, Wash.

1 Commander, New York Naval Shipyard, Naval Base, Brooklyn 1, N.Y.

1 Commander, Charleston Naval Shipyard, Naval Base, Charleston, S.C.

1 Commander, Pearl Harbor Naval Shipyard, Navy No. 128, Fleet Post  
Office, San Francisco, Calif.

1 Commander, Philadelphia Naval Shipyard, Naval Base, Philadelphia  
12, Pa.

1 Commander, Portsmouth Naval Shipyard, Portsmouth, N.H.

1 Commander, San Francisco Naval Shipyard, San Francisco 24, Calif.

1 Commander, Mare Island Naval Shipyard, Vallejo, Calif.





## TABLE OF CONTENTS

	Page
ABSTRACT . . . . .	1
INTRODUCTION . . . . .	1
THEORETICAL CONSIDERATIONS . . . . .	2
TEST METHODS . . . . .	7
RESULTS OF TESTS . . . . .	11
Characteristics of Records . . . . .	11
Notation . . . . .	13
Velocities . . . . .	15
Shock Wave Velocity $v_{o1}$ Versus Distance . . . . .	16
Final Maximum Velocity $v_{of}$ and Velocity Changes $\Delta v$ at Bubble Collapse Versus Distance . . . . .	20
Velocities of a Target under Water . . . . .	20
Initial Negative Acceleration . . . . .	23
Displacement and Long-Lasting Negative Acceleration . . . . .	23
Photographic Results . . . . .	24
Migration . . . . .	24
Maximum Bubble Radius . . . . .	24
Time Periods of Bubble Pulsation . . . . .	27
Cavitation . . . . .	31
CONCLUSIONS . . . . .	31
ACKNOWLEDGMENT . . . . .	33
REFERENCES . . . . .	33



THE RESPONSE OF SIMPLE FLOATING TARGETS  
TO UNDERBOTTOM EXPLOSION ATTACK

by

Erich Buchmann, Ph. D.

ABSTRACT

Underwater explosion tests have been conducted against simple cube-shaped floating wooden blocks, 10 x 11 x 10 inches and 20 x 20 x 20 inches. Charges were fired below the center of the blocks at distances from contact up to 10 feet. The charge weights varied from 1 gram to 90 grams.

The response of the targets was measured by recording the displacement, velocity, and in some cases the acceleration. High-speed motion pictures of the pulsation and migration of the gas bubble under water were taken simultaneously; these pictures also showed the occurrence of cavitation.

The response of the targets could be correlated with the different phenomena of the underwater explosions such as the shock wave, bubble pulses, cavitation, bubble expansion and contraction, and migration. The results are compared with theory and show that the response of the target resembles that of the water displaced by the target.

A few tests were made with a submerged target having the weight of the displaced water. The response also resembled that of the displaced water.

INTRODUCTION

The David Taylor Model Basin recently conducted a series of tests to measure the effect of underbottom explosion attacks on model targets.<sup>1</sup> The response of the targets to the explosions was measured by means of high-speed motion pictures taken at the surface and under water. These results showed clearly that too many details were lost, especially during the phases of the shock wave and bubble pulses.

It was, therefore, considered desirable to improve the time resolution of the target response by measuring not only the displacement but also the velocity and, if possible, the acceleration. As the total displacement of the targets for the charges used would range up to several inches, it was necessary to have a velocity meter which would allow for displacements of such

---

<sup>1</sup>References are listed on page 33.

magnitude. Furthermore, the velocity meter should not add too much weight to the target. A special bar-magnet velocity meter was developed to meet these conditions;<sup>2</sup> the displacement was measured with the retraction-type displacement gage.<sup>3</sup> The acceleration was measured at first with the commercially available Statham- and Massa-type gages,<sup>4</sup> but the results were so inconsistent that further use of these gages was abandoned. Instead, the acceleration was electrically derived from the velocity meter, only the negative acceleration of long duration between the bubble pulses being measured.

In these tests very simple wooden targets, floating on the surface, were used but the results exhibited so many interesting details that they were deemed worthy of a report.

### THEORETICAL CONSIDERATIONS

The effect of underwater explosions upon a target depends on the interaction of the generated pressures and particle velocities in the surrounding water with the target.<sup>5,6</sup> The detonation of the explosive creates a shock wave in the water accompanied by high pressures. The first high-pressure part may be followed by a much lower pressure of long duration. At the same time the gas bubble expands and contracts. The pressure around the bubble decreases with increasing expansion of the gas bubble and may be negative for an appreciable time. The contraction of the gas bubble increases the pressure, which becomes positive as the bubble contracts more and more. This pulsation of the gas bubble may occur several times. Figure 1 is a diagram illustrating these underwater-explosion phenomena. The pressure in the shock wave is high, but its duration is very short compared with that of the later phenomena. It may, therefore, be possible that the later stages with low or even negative pressures have a considerable effect on the target because these pressures act over a long time interval.

When the target is floating, the pressure field is not only modified by the target but also by the free surface of the water, which is usually taken care of by calculating the effect of an image of the charge in the surface of the water.

In the tests described in this report, the targets consisted essentially of wooden blocks with nearly the same acoustical impedance as water. The shock wave, therefore, will penetrate the target and travel to its upper surface. A thin sheet of steel was fastened to the bottom of the blocks; but it can be shown that this would only distort the wave without altering its total impulse. At the surface of the block the shock wave will then be reflected and, as the pressure at the surface is zero, a tension wave will travel back. If no cavitation occurs, this tension wave travels back into the

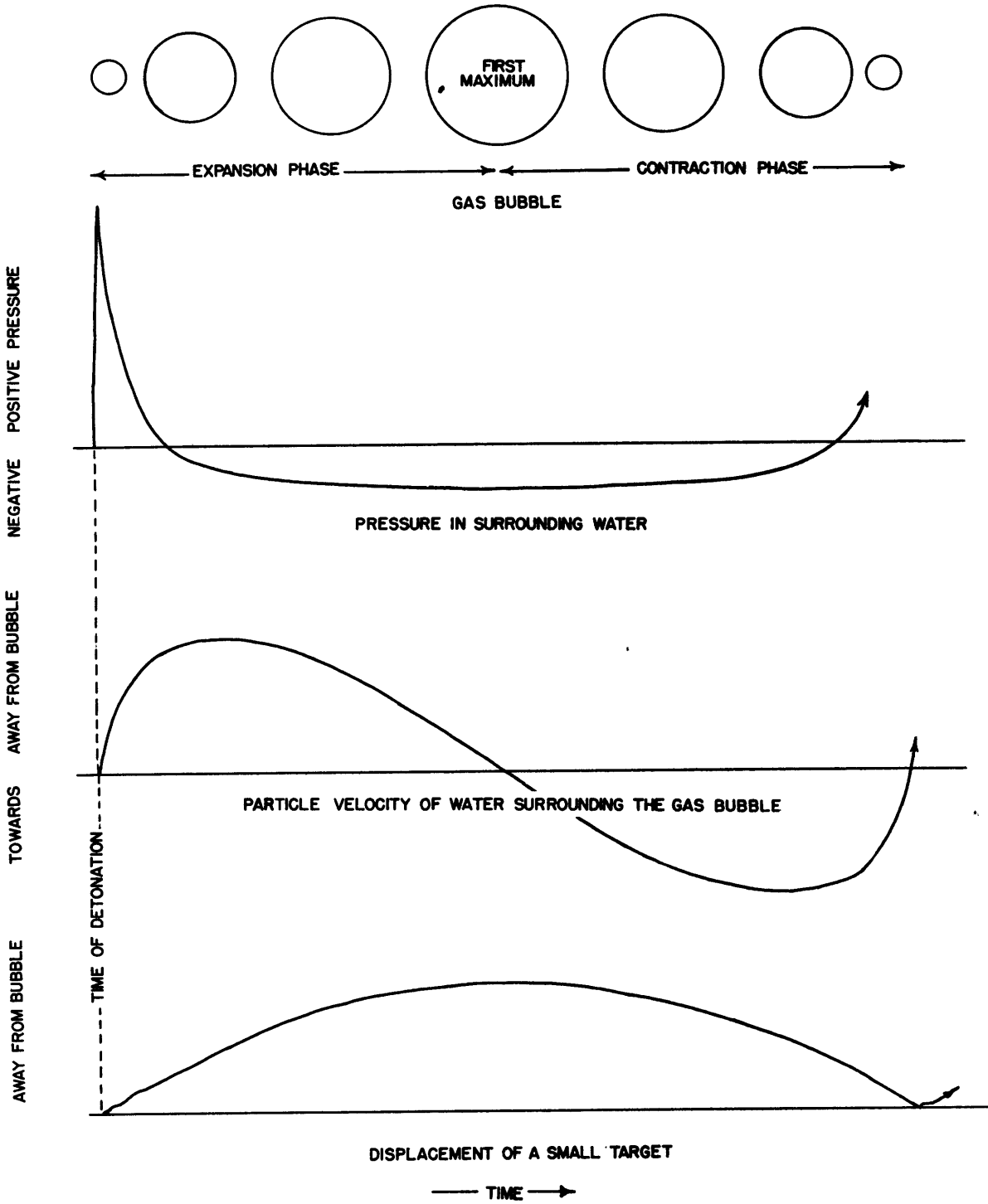


Figure 1 - Diagram Illustrating Some Underwater-Explosion Phenomena



water, leaving the target without motion and with a final displacement. In such a case a velocity meter would record velocity only during the time of the passage of the shock wave.

If the water below the block cannot withstand the tension of the reflected wave, cavitation may be observed below the block. In that case, the shock wave will travel vertically back and forth through the block and cause an upward motion of the block, retarded by the difference between atmospheric pressure and the lower pressure in the cavitated region. A velocity meter combined with a string galvanometer will measure, in these cases, the mean upward motion of the block retarded by the cavitation.

The cavitation will then be closed up by the outrush of water caused by the gas-bubble expansion. The particle velocity of the water in this stage will depend on the rate of expansion of the gas bubble and will decrease inversely with the square of the distance. The velocity of the target during this stage will therefore decrease more rapidly with increasing charge distance than the initial velocity due to the shock wave.

In the case of a submerged target having the same acoustical impedance as water, on the other hand, the shock wave merely travels through the target and passes on into the water above it. The target would then come to rest, being displaced a small amount. In this case no cavitation will occur, and later the target may follow the outrushing water as the gas globe expands.

For the target at the surface an additional effect due to the reflected shock wave at the water surface has to be considered. This tension wave may cause the water to cavitate to a certain depth below the surface. For the targets used during these tests, however, the reflected waves in the target and in the water arrive at the bottom of the target at nearly the same time, so that no release pressure is to be expected in addition to the actions already mentioned.

From these considerations, it is to be expected that the shock wave will first impart a certain velocity to the target, then this velocity will decrease to a minimum, after which the target should follow the average water motion, its velocity increasing to a second maximum and then decreasing.

The initial velocity due to the shock wave can perhaps be estimated in the following way. If  $p$  denotes the pressure in the shock wave, the impulse on unit area of the target is  $\int p dt$ . Now  $\int p dt$  is also the impulse per unit area in the shock wave and has the value, at a distance of  $r'$  feet from a charge of weight  $W$  pounds,

$$\int p dt = CW^{2/3} \frac{1}{r'} \text{ lb-sec/in}^2$$

where  $C$  is a constant. The total impulse  $I_t$  delivered to the target is obtained by integrating over the whole bottom area. To simplify the calculation, the bottom will be replaced by a circle of the same area. If  $r$  denotes the radius of this circle and  $D$  the distance of the charge below the center of the circle, both in inches, then at a distance  $x$  inches from the center,

$$r' = \frac{\sqrt{D^2 + x^2}}{12}$$

and

$$I_t = 12 CW^{2/3} (2\pi) \int_0^r \frac{x dx}{\sqrt{D^2 + x^2}} = 75.5 CW^{2/3} [\sqrt{D^2 + r^2} - D] \quad [1]$$

Let

$$n = \frac{D}{r}$$

Then, in nondimensional form,

$$\frac{I_t}{75.5 CW^{2/3} r} = \sqrt{n^2 + 1} - n$$

Now, if  $M$  is the mass of the target and  $v_{oi}$  the velocity imparted to it by the shock wave,

$$M v_{oi} = I_t$$

Hence

$$v_{oi} = \frac{1}{M} 75.5 CW^{2/3} r [\sqrt{n^2 + 1} - n] \quad [2]$$

The value of  $C$  used in this report for pressed tetryl is 1.77; that for PETN, 2.2. The masses of the targets were 0.84 and 5.13 slugs, and the effective radii 5.92 and 11.3 inches, respectively.

During the subsequent expansion of the gas globe, the radial particle velocity  $u$  of the water reaches a maximum after a time of about 12 percent of the bubble period. This maximum particle velocity  $u_{\max}$  can be expressed with sufficient accuracy in terms of the maximum bubble radius  $R_m$ . At a fixed distance  $D$  from the center of the gas globe,

$$u = \frac{R^2}{D^2} \frac{dR}{dt}$$

where  $R$  denotes the instantaneous radius of the gas globe. Ignoring the small pressure in the gas globe so that Equation [14] and, as valid for large oscillations, Equation [20] in Reference 7 can be used,

$$R^2 \frac{dR}{dt} = R^2 \sqrt{\frac{C_0}{R^3} - \frac{2}{3} \frac{P_0}{\rho}}$$

and

$$C_0 = \frac{2}{3} \frac{P_0}{\rho} R_m^3$$

which gives a maximum value of  $u$  at  $R = \frac{R_m}{4^{1/3}} = 0.63 R_m$ . Using this value, we obtain

$$u_{\max} = 18.55 \frac{R_m^2}{D^2} \left(1 + \frac{H}{34}\right)^{1/2} \quad [3]$$

where  $H$  is the depth of the charge below the water surface in feet.

It is interesting to compare the motion of the target during this stage with the average upward particle velocity that the volume of water displaced by the target has, when the target is not there. For simplicity, however, this average was calculated only along a horizontal plane drawn through the block at mid-draft, or, for charges close to the block, over two such planes, at one-quarter and three-quarters draft. The actual average would differ only slightly. Over such a plane at a height  $D_1$  above the target, the average maximum vertical particle velocity due to symmetrical outflow from the gas globe is, in the notation used for the shock wave,

$$\bar{u}_1 = 18.55 R_m^2 \frac{2\pi D_1}{\pi r^2} \int_0^r \frac{x dx}{\sqrt{(D_1^2 + x^2)^3}} \left(1 + \frac{H}{34}\right)^{1/2}$$

or

$$\bar{u}_1 = 18.55 \left(1 + \frac{H}{34}\right)^{1/2} R_m^2 \frac{2}{r^2} \left[1 - \frac{D_1}{\sqrt{D_1^2 + r^2}}\right]$$

or, replacing  $D_1$  by  $n_1 r$ ,

$$\bar{u}_1 = 18.55 \left(1 + \frac{H}{34}\right)^{1/2} R_m^2 \frac{2}{r^2} \left[1 - \frac{n_1}{\sqrt{n_1^2 + 1}}\right] \quad [4]$$

A second similar term is then to be added to represent flow toward the image of the gas globe in the free surface of the water. If  $D_1 = m_1 r$  is the distance of the image from the chosen horizontal plane, we obtain

$$\bar{u} = 18.55 R_m^2 \frac{2}{r^2} \left(1 + \frac{H}{34}\right)^{1/2} \left[2 - \frac{n_1}{\sqrt{n_1^2 + 1}} - \frac{m_1}{\sqrt{m_1^2 + 1}}\right] \quad [5]$$

This equation leads to the nondimensional form

$$\frac{\bar{u} r^2}{18.55 R_m^2 2 \left(1 + \frac{H}{34}\right)^{1/2}} = 2 - \frac{n_1}{\sqrt{n_1^2 + 1}} - \frac{m_1}{\sqrt{m_1^2 + 1}} \quad [6]$$

After reaching a maximum, the average upward particle velocity will decrease and pass through zero at the time of maximum diameter of the bubble. The particle velocity will then continue to decrease to a negative maximum, or greatest downward velocity, equal in magnitude to the first maximum upward velocity; this value is attained at a little less than 90 percent of the bubble period from the start.

Formulas for the average displacement and acceleration of the water could also be deduced for comparison with observed values, but the comparison with the velocity measurements, which are the most accurate, will suffice.

During subsequent pulsations of the gas globe, further pulses of pressure are emitted, which have similar effects on the target. The magnitude of these effects will depend on the position of the bubble at this time, which may differ from the original position because of migration.

#### TEST METHODS

After several trials the test arrangement shown in Figure 2 was selected; with this setup, displacement, velocity, and electrically derived long-duration negative acceleration of simple wooden blocks were measured. One velocity meter was used only for recording velocities, while a second velocity meter was used only for measuring accelerations.

Two Alnico-V permanent magnets, 6 inches long and 3/8 inch in diameter, protected by a thin copper tube, were mounted on the top of the wooden block. Both magnets were inserted in coils, so that the linear output range covered a displacement of 4 inches. The coils were seismically suspended to a framework, which was itself mounted to a rigid platform. The displacement-gage wire was connected to the center of the block.

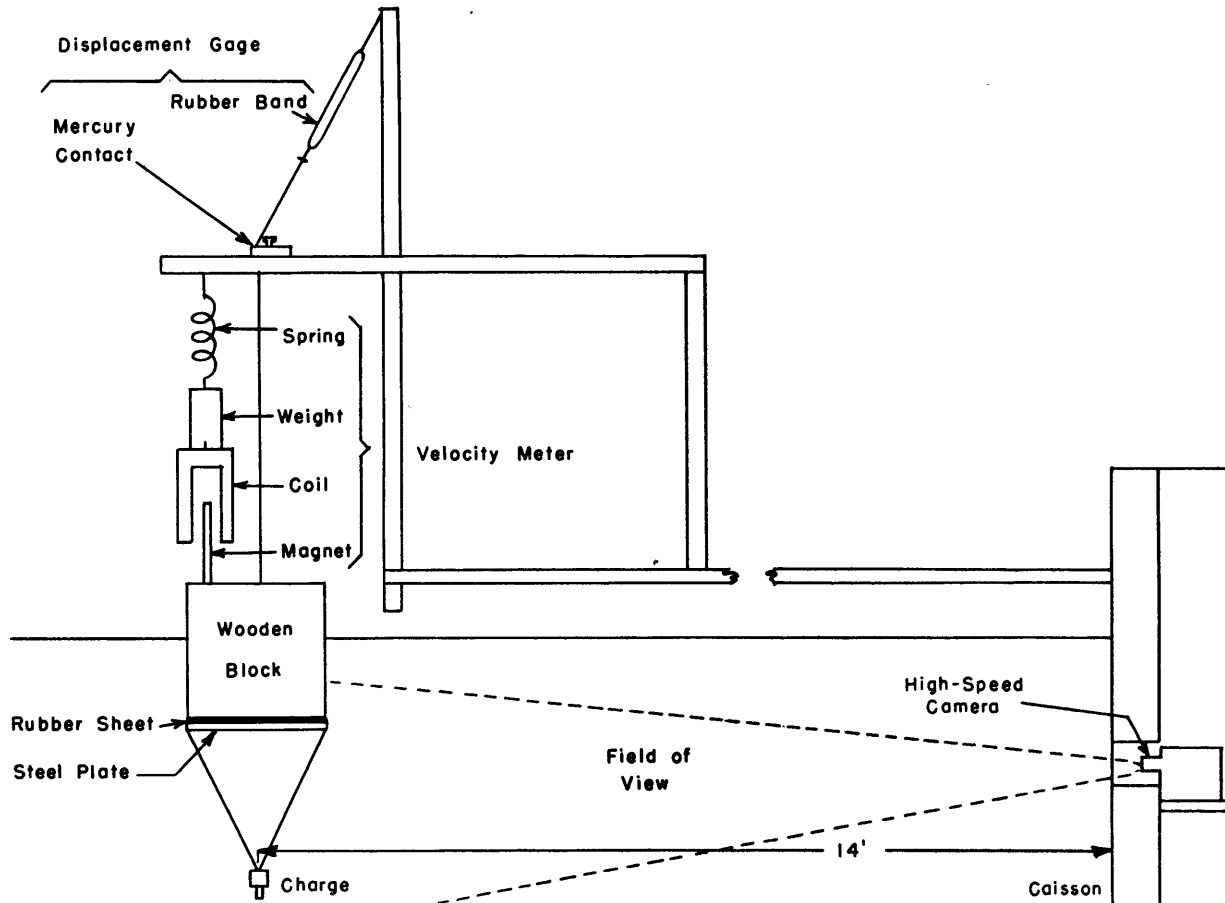


Figure 2 - Schematic Diagram of Test Arrangement

A 16-millimeter Eastman high-speed camera was mounted in a caisson, 14 feet from the block, so that the field of view covered the area from the surface to a depth of about 4 feet. For charges at greater depths, a second camera with a special wide-angle lens<sup>8</sup> covered the area up to a 10-foot depth. The timing on the film was marked by a specially built 1000-cycles per second timing-pulse generator, DTMB Type 61A,<sup>9</sup> which also is equipped with a zero-time marker, using as zero indicator the trigger gage developed by the Norfolk Naval Shipyard.<sup>10</sup> In this way, the arrival of the shock wave at the bottom of the target was marked on the film.

The wiring diagram is shown in Figure 3. The coil for the velocity meter consisted of two layers of H.F. Formex magnet wire, 0.0159 inch in diameter, wound on a polystyrene tube 12 inches long and 1.75 inches in inside diameter. The coil had a resistance of 24 ohms. The output of this velocity meter was 128 millivolts per foot per second. The coil was connected to a



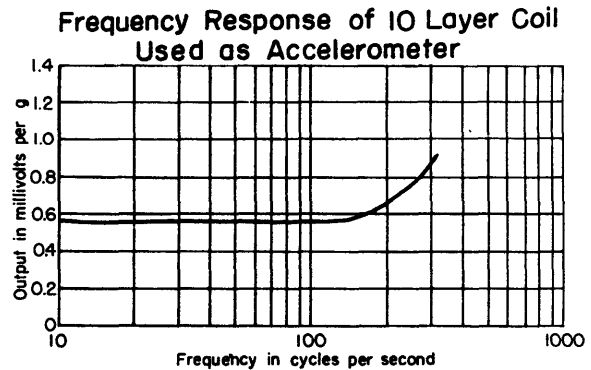
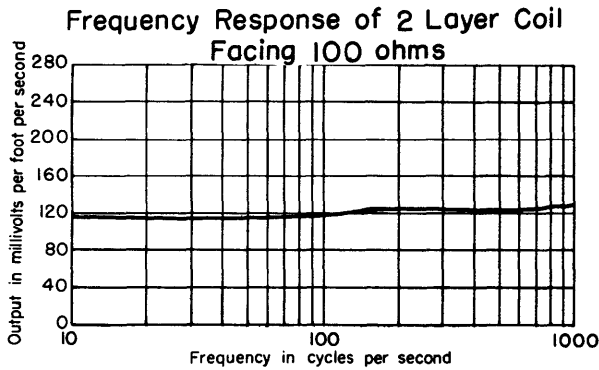
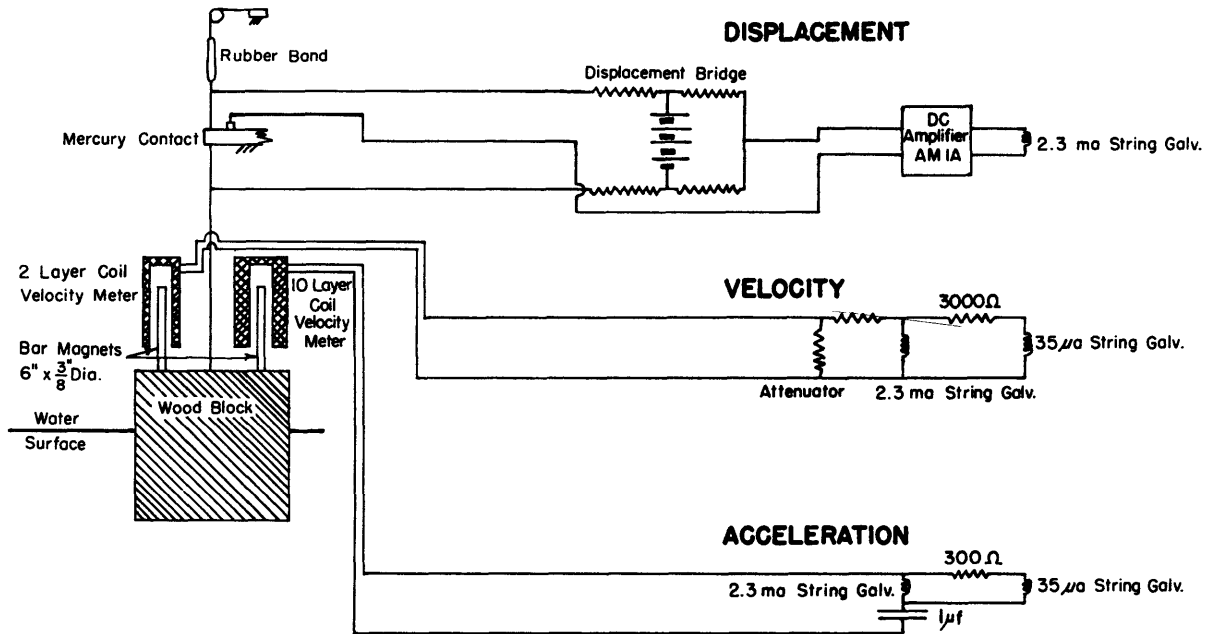


Figure 3 - Wiring Diagram of Test Arrangement

The velocity readings obtained with the 35-microampere galvanometers were not used.

2.3-milliampere galvanometer string of a 36-channel Consolidated oscillograph through an attenuator box. As the frequency response of the velocity meter depends on the connecting impedance, the attenuator resistances were arranged in such a way that the velocity-meter output always faced the same resistance of 100 ohms. The frequency response of the meter is shown in Figure 3. As the galvanometer has a natural frequency of about 800 cps and fluid damping of about 0.6 critical, the frequency response should be uniform up to about 480 cycles per second.

The long-duration negative acceleration was derived from a 10-layer coil wound on a 2-inch diameter brass tube, 12 inches long. The coil resistance was about 40 ohms. The output was connected to a 2.3-milliampere galvanometer in series with a 1-microfarad capacitor. A 35-microampere galvanometer string in series with 300 ohms was connected in parallel with the 2.3-milliampere galvanometer. The frequency response of this arrangement is also shown in Figure 3 and is flat up to 130 cycles per second. The output of the derived acceleration was 0.58 millivolts per g.

The wide inside diameter of both coils allowed free motion of the magnets thus preventing undesirable friction. Both coils were screwed to a weight of 25 pounds and seismically mounted with a natural frequency of 1.5 cycles per second.

The retraction-type displacement gage consisted of Nichrome-V wire (Number 28 B and S gage) and was stretched by a rubber band with a tension of 5 pounds. The gage was in one arm of a Wheatstone bridge. The output was amplified by an AM1A d-c amplifier and was recorded by a 2.3-milliampere galvanometer.

Two targets were used for the test. The large wooden block was 20 x 20 x 20 inches. The bottom was protected against the explosions by a 3/8-inch steel plate 20 x 20 inches in area which was fastened by 81 screws each 4 inches long. A rubber sheet, 1/4 inch thick and 20 x 20 inches in area, was between the steel plate and the block. The small block was 10 x 11 x 10 inches with a 3/16-inch steel plate at the bottom and a 1/8-inch rubber sheet between the steel plate and the block. The weight of the large block was 165 pounds; that of the small one 27 pounds, including instrumentation.

The following charges were used for the tests:

a. Hercules Engineer Special detonator consisting of 1.00 gram of PETN and 0.41 gram of booster consisting of diazodinitrophenol and 25 percent potassium chlorate, the total charge being equivalent to 1.24 grams of PETN.

b. 8 grams pressed tetryl pellets, detonated by a Number 8 cap, equivalent to 8.50 grams of tetryl.

c. 90 grams of PETN plus 5 percent wax, detonated by a Number 8 cap, equivalent to 90 grams of PETN.

The equivalent weights were derived from underwater photographs and checked with other test results.<sup>11</sup>

All charges were suspended by strings below the center of the targets. The distance from charge to target was measured from the bottom of the target to the center of the charge.

After the charge was in proper position, the sequence of the test was as follows: The camera was started, and a microswitch set off a sequence timer, Type 74A,<sup>12</sup> which in turn controlled the background illumination for the camera field and fired the charge with 30 milliseconds delay. At the same time the oscillograph used for recording the outputs of the various gages was started.

## RESULTS OF TESTS

### CHARACTERISTICS OF RECORDS

A typical oscillograph record is shown in Figure 4. It was obtained in a test in which a charge of 8 grams of pressed tetryl was detonated with a Number 8 cap at 40 inches below the small block. The upper three records were taken with low-frequency-response galvanometers. The galvanometers for the lower five records have a flat frequency response up to 480 cycles per second.

The velocity record in Figure 4 shows a large initial rise which drops and rises once more to a second maximum. Thereafter the velocity drops continuously to a maximum negative velocity. Then a sudden change to a maximum positive velocity occurs at the time of the bubble collapse. A similar pattern follows during the second bubble pulsation, and several further oscillations can be observed, the change in velocity becoming progressively smoother.

The displacement shows a small initial value, followed by a hesitation and then increases to a maximum. Thereafter it drops practically to zero and begins to increase once more at the first bubble collapse. Several similar patterns occur during the subsequent pulsations of the bubble.

Only the value of the maximum negative acceleration was taken from the acceleration record. This value was measured at the middle of the various pulsation periods.

An assembly of velocity records obtained from charges of 8 grams of pressed tetryl detonated with a Number 8 cap below the large block, at various distances between 5 and 60 inches, is shown in Figure 5. All curves start with an initial high velocity, drop afterwards, reach a second maximum, and drop to a maximum negative velocity crossing the zero line at the same time at

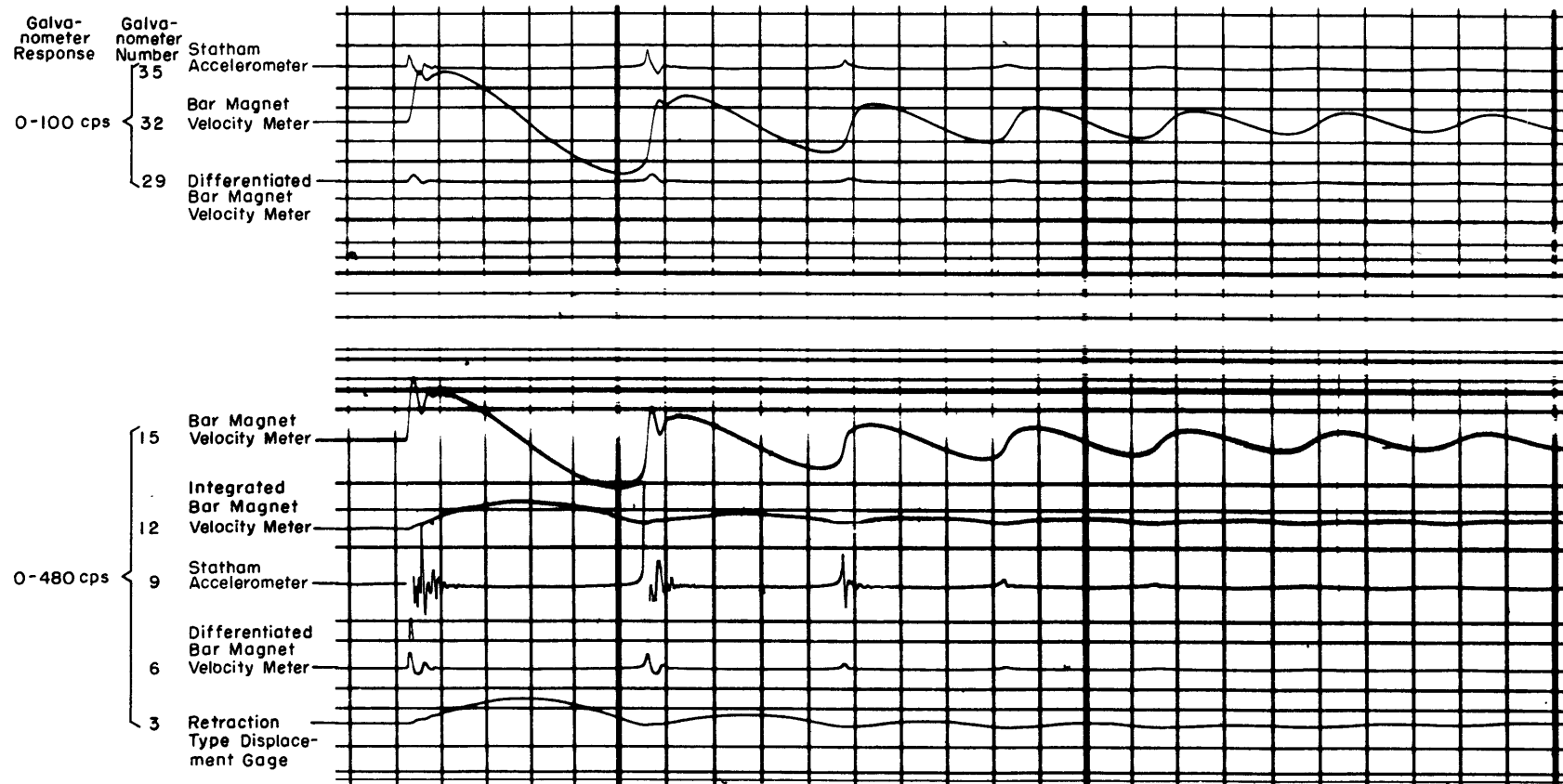


Figure 4 - Typical Oscillograph Record

Statham accelerometers were used only during the exploratory phase of the tests.

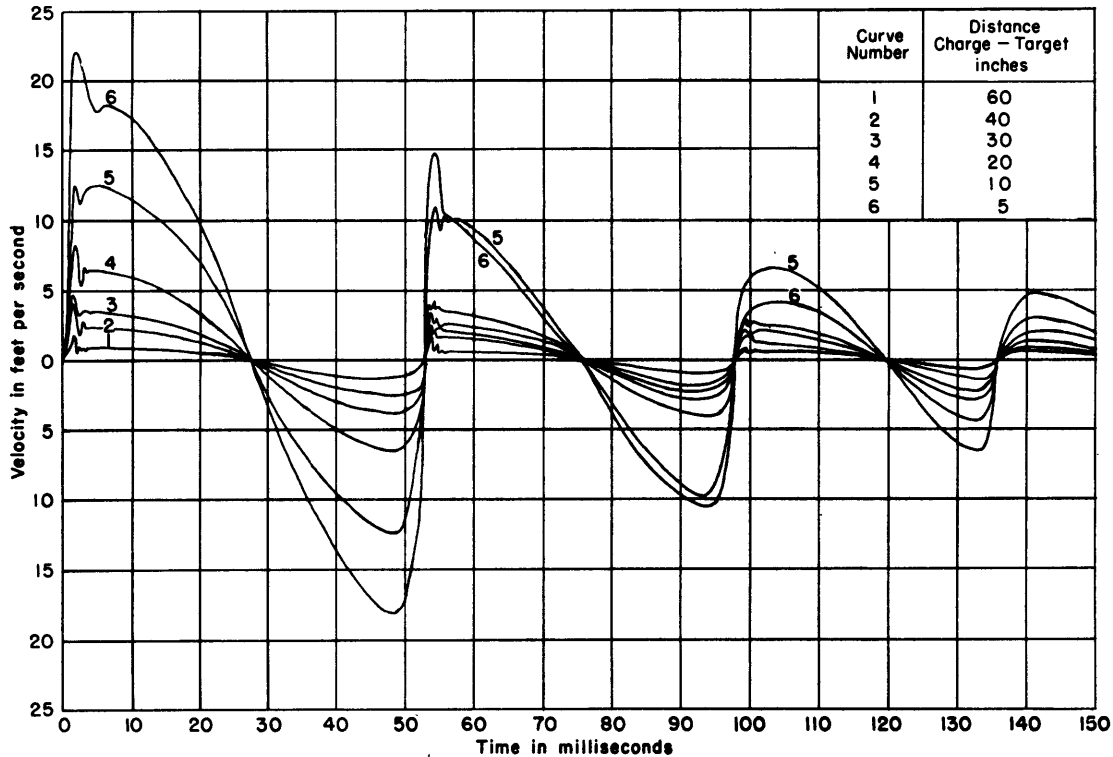


Figure 5 - Velocity Records of Large Block for Charges at Indicated Distances

All charges were 8 grams of tetryl with a Number 8 cap.

the middle of the pulsation period. The curves for charges closer to the target show a smoother pattern during the initial stage than those for remote charges.

#### NOTATION

In discussing the data, a standard terminology will be useful. Figure 6 shows a diagram for the displacement, velocity, and acceleration records obtained during these tests with examples of the notation. The notation used is:

- $d_j$  Displacement in inches. Index refers to number of pulsations of the gas globe, using 0 for the initial stage.
- $v$  Velocity in feet per second. First index refers to number of pulse using 0 for the initial stage. Second index refers to a particular velocity during a pulsation. Index  $i$  is initial velocity,  $f$  is final maximum positive velocity, and  $n$  is maximum negative velocity.



$$\Delta v_j = v_{(j-1)n} + v_{jf}$$

where j denotes the particular bubble pulse involved, and j is one for the first pulse.

a Acceleration in g. Where one index is used, the acceleration is the maximum negative value for a particular pulse cycle with 0 referring to the initial expansion. Where two indices are used the first one denotes the cycle and the second one refers to a particular one of several peak positive accelerations during one pulse.

t Period in milliseconds. One index refers to the period of the indicated pulsation. The first of two indices is used as for the velocities. The second refers to a particular one of several peak accelerations during one pulse.

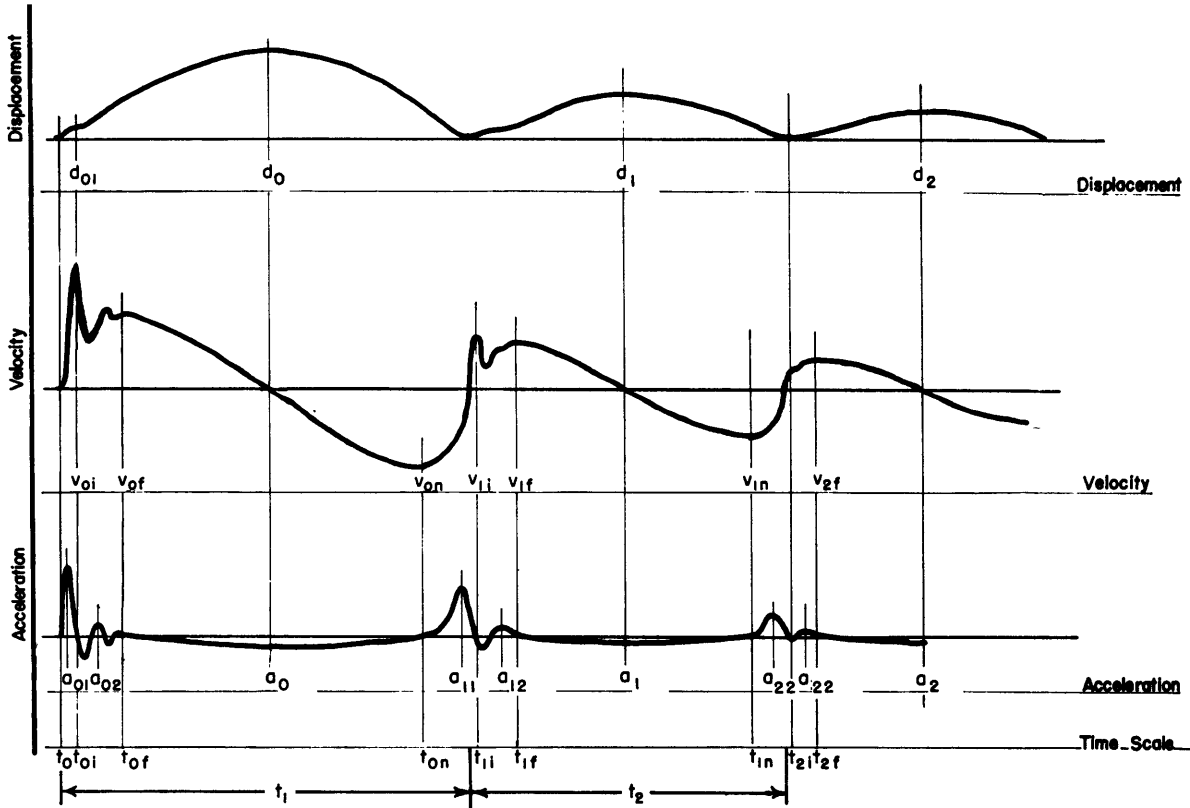


Figure 6 - Notation Used for Displacements, Velocities and Accelerations

## VELOCITIES

A series of tests were conducted with each type of charge against both targets at distances ranging from contact up to 120 inches. It was found that the final peak positive velocity was equal to the following peak negative velocity during all pulsations.

Figure 7 shows a plot of the final peak velocity  $v_{of}$  and also  $\Delta v_j$  versus distance for a charge of 8 grams of pressed tetryl with a Number 8 cap fired below the large block at distances from 5 inches up to 100 inches. The curve for  $\Delta v_1 = v_{on} + v_{1f}$ , the velocity change at the first bubble pulse, shows the largest values for all distances. The curve for the final maximum velocity  $v_{of}$  has nearly the same slope, but the values are considerably less than those for  $\Delta v_1$ . The curves for the velocity changes at the second and later bubble collapses represent lower values and exhibit somewhat different slope.

In Figure 7 the response to the various pulses seems to exhibit a relative minimum at 15 inches and a relative maximum at 30 inches. This effect is obviously caused by the migration of the bubble either toward or away from the target. The graph in Figure 7 is, therefore, replotted in Figure 8 with a correction for the distances of the bubble from the target, based on the migration measurements. The result is a set of parallel curves for the

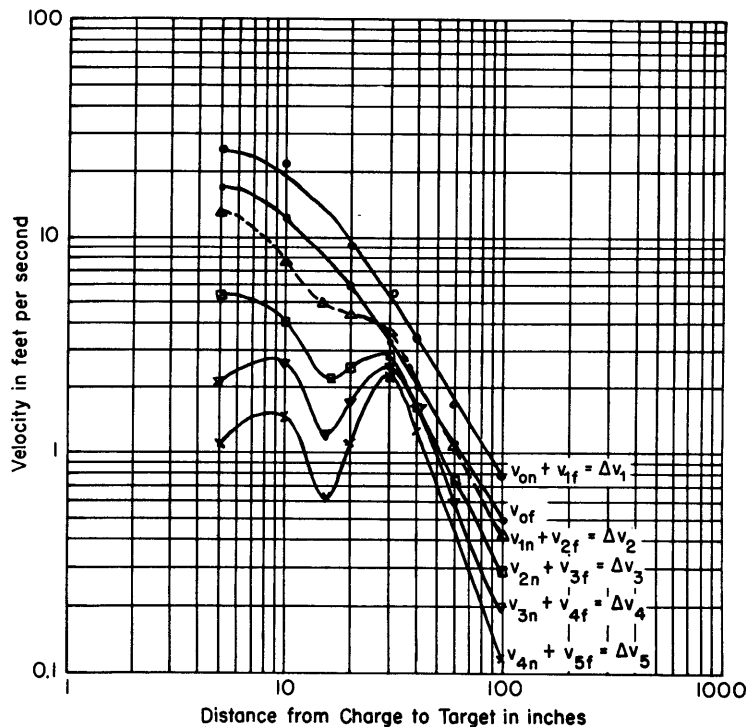


Figure 7 - Velocities of Large Block, without Correction for Migration, for Charge of 8 Grams of Pressed Tetryl with Number 8 Cap

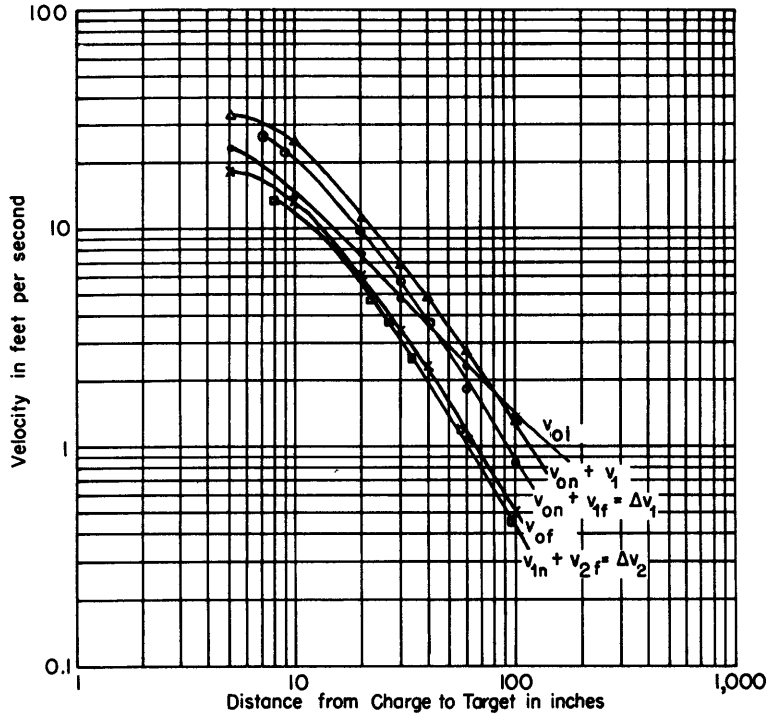


Figure 8 - Velocities of Large Block, Corrected for Migration, for Charge of 8 Grams of Pressed Tetryl with Number 8 Cap

change in velocity at the various bubble collapses showing, at a given distance, decreasing values in the sequence  $\Delta v_1$ ,  $v_{of}$ ,  $\Delta v_2$ ,  $\Delta v_3$ .

Figure 8 includes also the curve for the initial peak velocity  $v_{0i}$ . The slope of this curve differs from all the other curves and corresponds to a much slower decrease with increasing distance.

Similar curves corrected for migration are plotted for the other series of tests in Figures 9 through 12.

#### Shock Wave Velocity $v_{0i}$ Versus Distance

The values of all measured initial peak velocities  $v_{0i}$  are plotted in Figure 13 versus distance from charge to target. It can be seen that in general the slope of all curves is the same and represents variation inversely proportional to the distance.

A comparison of these measured velocities with those calculated from the impulse of the shock wave according to Equation [2] is shown in the non-dimensional plot of Figure 14. The curve drawn in the figure is calculated, and the points are derived from all measurements. The points follow the curve at large distances, but deviate to slightly higher values for closer distances, and show nearly twice the calculated value at very close range. A possible

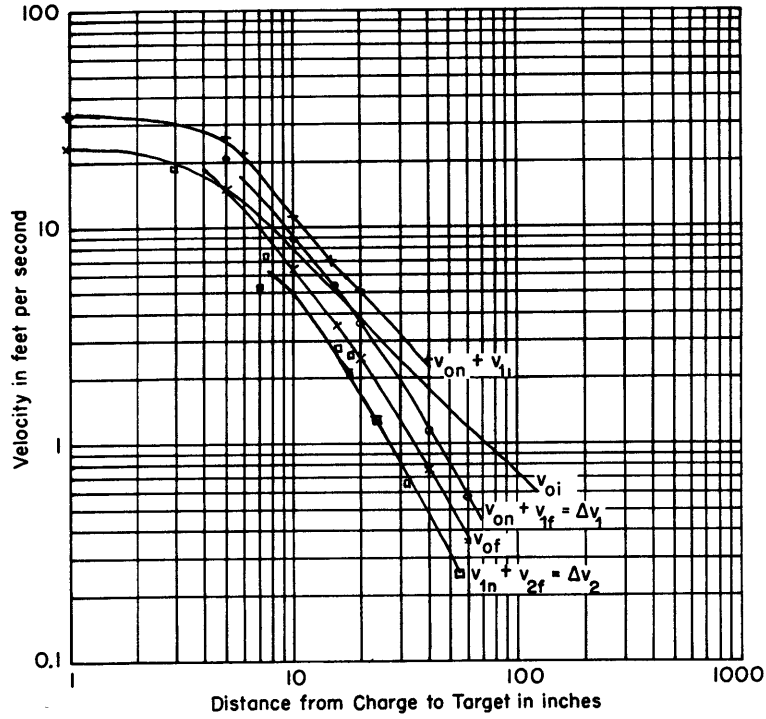


Figure 9 - Velocities of Small Block, Corrected for Migration, for Hercules Engineer Special Detonator Cap

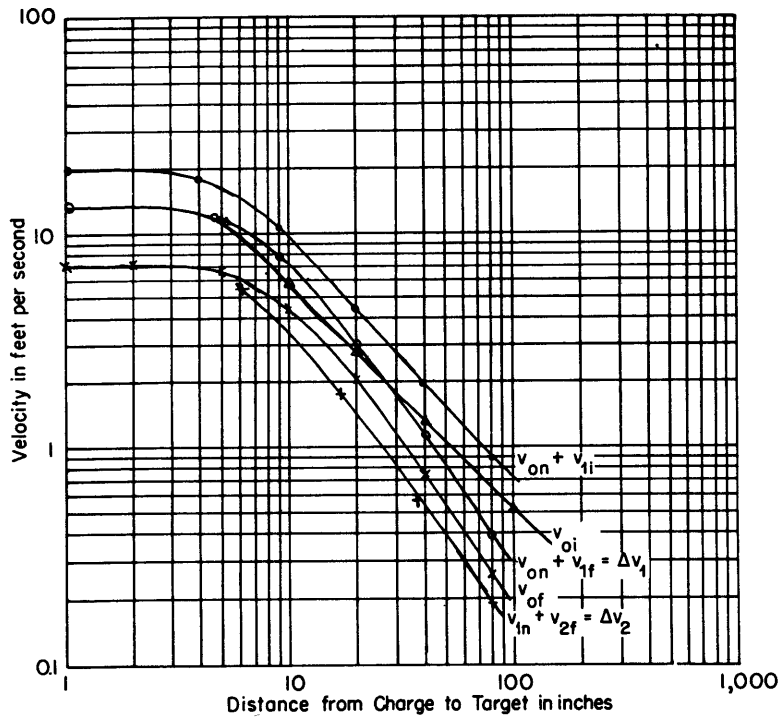


Figure 10 - Velocities of Large Block, Corrected for Migration, for Hercules Engineer Special Detonator Cap

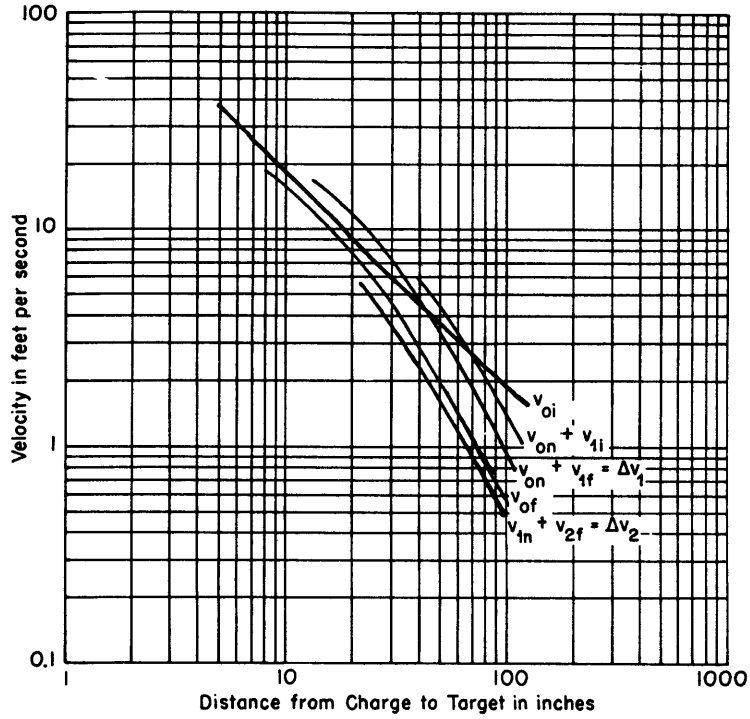


Figure 11 - Velocities of Small Block, Corrected for Migration, for Charge of 8 Grams of Pressed Tetryl with Number 8 Cap

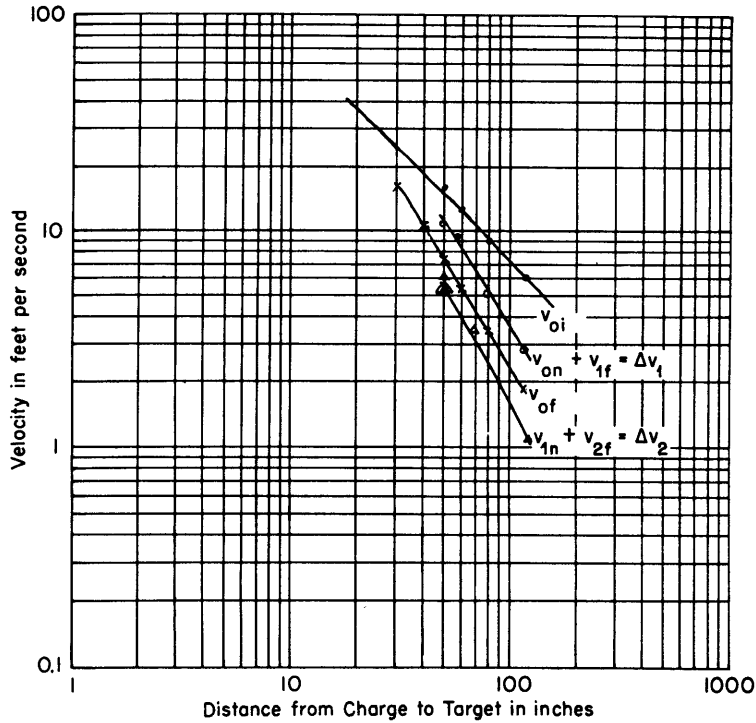


Figure 12 - Velocities of Large Block, Corrected for Migration, for Charge of 90 Grams of PETN with Number 8 Cap



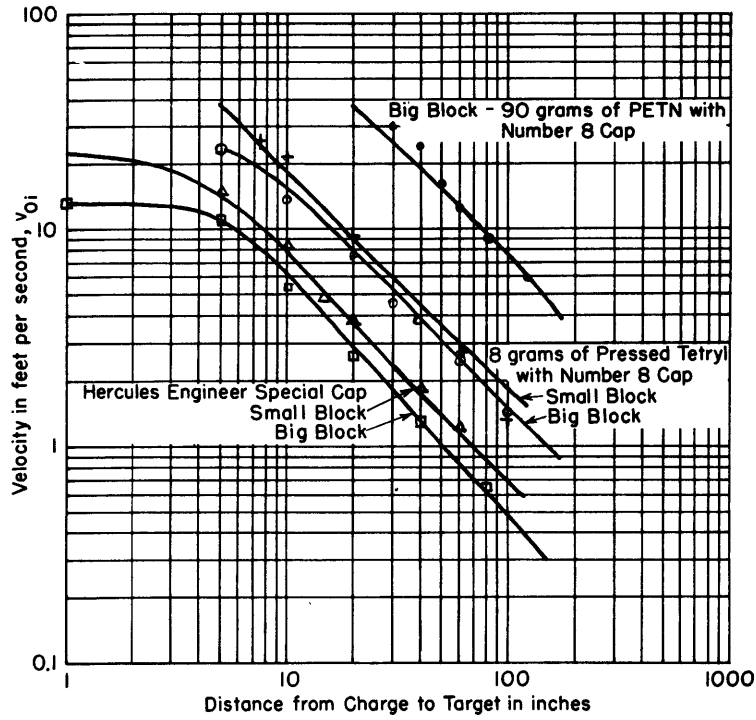


Figure 13 - Initial Velocity Versus Distance for Indicated Targets and Charges

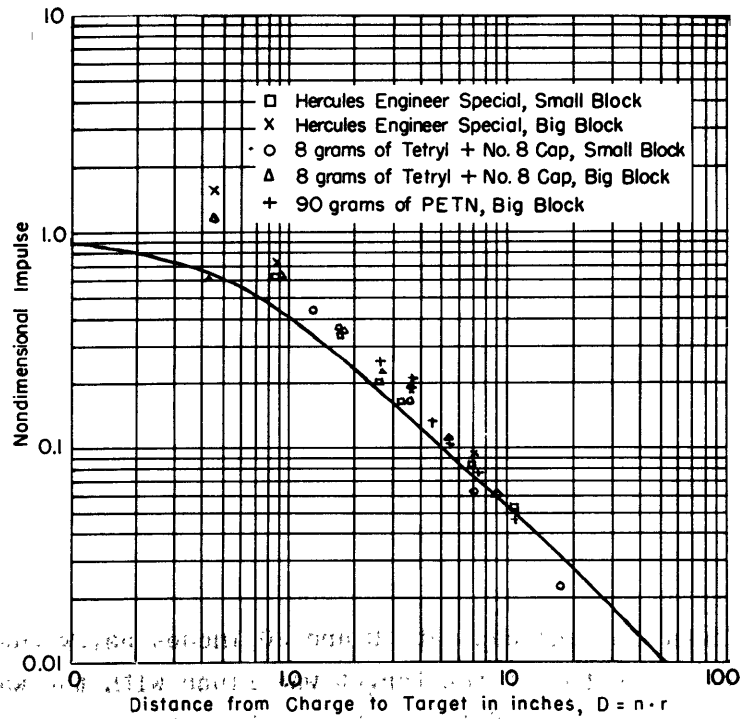


Figure 14 - Nondimensional Plot of Impulse Versus Distance for Shock Wave

Here  $D$  is the distance from charge to target in inches,  
 $r$  is the radius of a circle with the same area as the target bottom in inches, and  
 $n$  is equal to  $D/r$ .

The curve is a plot of  $\sqrt{n^2 + 1} - n$ . The points are impulses reduced in accordance with Equation [2].

explanation of this deviation is as follows: At close distances the acceleration of the block as a whole is much less than that of the water near the charge when the block is replaced by water, hence partial reflection of the shock wave occurs and the impulse given to the block is thereby increased.

Final Maximum Velocity  $v_{0f}$  and Velocity Changes  $\Delta v$  at Bubble Collapse Versus Distance

The final maximum initial velocity of the target occurs after a little more than 10 percent of the bubble period. At this time the target would have come to rest through the action of underpressure if the shock wave were a plane wave. A spherical wave, however, leaves the water moving outward in association with the expansion of the gas bubble. Since the subsequent maximum velocity of the water as the gas globe expands occurs nearly at the same time that the target attains its final maximum velocity, it may be imagined that during the next phase the target will closely follow the particle velocity of the water. The average particle velocity of the water displaced by the target may therefore be calculated according to Equation [6] and compared with the velocity response of the target. This is the more justified because the maximum negative velocity of the target is equal in magnitude to the final peak positive velocity; this is also true for the particle velocity.

Average maximum velocities of the displaced water calculated from Equation [6] are shown by the curve in Figure 15, the measured velocities being indicated by points. It can be seen that the observed points follow the calculated lines very closely, even at small distances. A nondimensional plot exhibiting this comparison for all measured values is shown in Figure 16.

The ratio of the velocity change  $\Delta v_j$  due to a bubble pulse to the final maximum velocity  $v_{0f}$  is plotted for successive bubble pulses in Figure 17. This ratio is a constant for any given distance of the collapsing bubble from the target.

Velocities of a Target under Water

A few tests were conducted with a target which had the same average density as the water and the dimensions of the small block. The charges used were Hercules Engineer Special caps at 10 and 20 inches below the bottom of the target. In one test, the top of the target was flush with the water surface; in the second test the top was 18 inches below the water surface. Only velocities were measured in these tests.

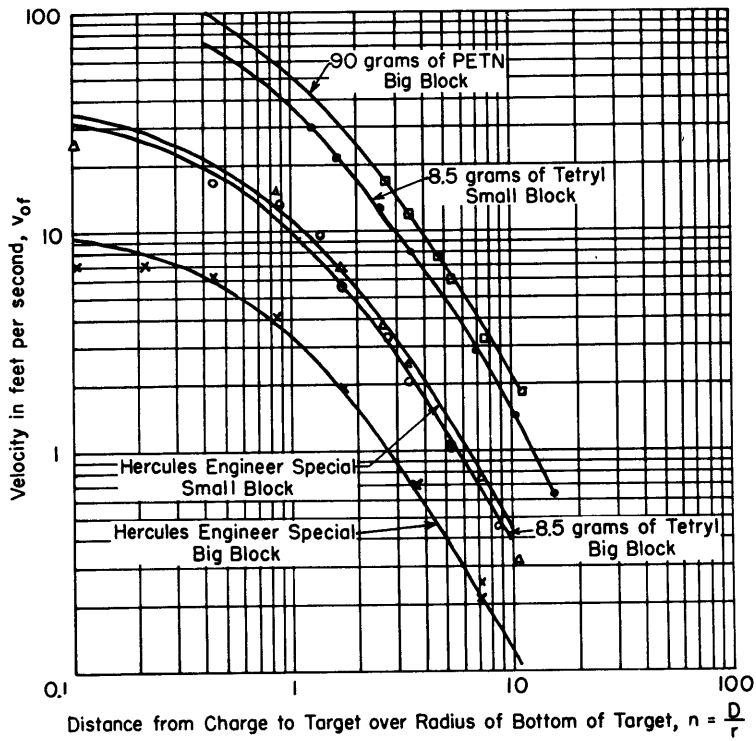


Figure 15 - Particle Velocity of Displaced Water Compared with Target Velocity

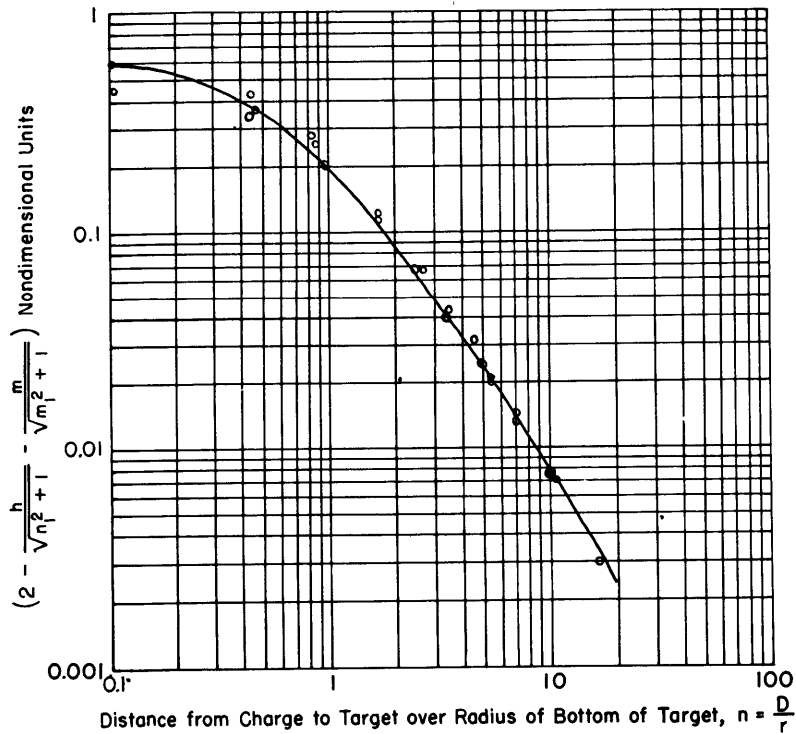


Figure 16 - Nondimensional Plot of Target Velocity Compared with Calculated Particle Velocity of the Displaced Water

Data for large and small blocks are included. The points correspond to measured velocities reduced to the nondimensional form of Equation [6].

The records obtained show a markedly decreased effect of the shock wave; presumably the shock wave was transmitted through the block to the water on the far side. The velocity rises to the final maximum velocity with only a few small wiggles at the very beginning. A similar pattern was observed at the bubble pulses. The history of the velocity is otherwise very similar to that obtained from the targets at the surface. The measured values for the final maximum velocity are given in Table 1 and are compared with the calculated average particle velocity of the displaced water.

TABLE 1

Comparison of Calculated Average Particle Velocities with Measured Velocities for Small Block Under Water

The charge was a Hercules Engineer Special Cap.

Position of Target	Distance, Charge to Target inches	Final Maximum Velocity feet per second	
		Measured	Calculated
Flush with Water Surface	10	5.62	5.65
	20	2.36	2.40
Top 18 inches below Water Surface	10	4.0	4.35
	20	1.73	1.83

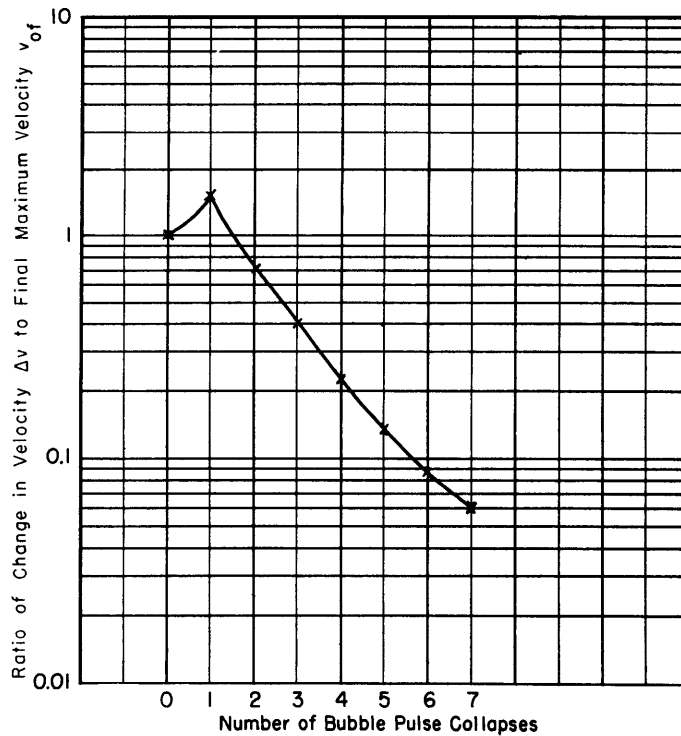


Figure 17 - Ratio of Change in Velocity  $\Delta v$  at Bubble Collapses to Final Maximum Velocity  $v_{of}$

These results show that a target flush with the surface or even entirely submerged also follows the motion of the water it displaces.

#### INITIAL NEGATIVE ACCELERATION

After the initial peak velocity caused by the shock wave, a steep drop in velocity occurs for a short time. The underwater pictures show cavitation during this period. The decrease in velocity was measured for one series of tests made with 8 grams of pressed tetryl against the large block; duration estimates being taken from the high-speed motion pictures and the oscillograph records. From these data the average deficit of pressure below hydrostatic pressure that must have been acting on the bottom of the target during this period was calculated; the results are listed in Table 2.

TABLE 2

#### Deficit of Pressure Acting on Large Block during First Cavitation

The charge was 8 grams of pressed tetryl with a Number 8 cap.

Distance, Charge to Target inches	Calculated Deficit of Pressure pounds per square inch
60	9.75
40	11.8
30	11.0
20	9.45
10	16.2
5	14.3

These values are very crude, as the time resolution is not very accurate, but they indicate that there must have been nearly a vacuum below the target during this period.

#### DISPLACEMENT AND LONG-LASTING NEGATIVE ACCELERATION

The maximum displacements of the target, denoted by  $d_0$ ,  $d_1$ ,  $d_2$ , in Figure 6, and the long-lasting negative accelerations denoted by  $a_0$ ,  $a_1$ ,  $a_2$ , were measured for certain of the tests. They confirm the results obtained from velocity measurements and agree with the calculated values and will, therefore, not be shown in detail.

## PHOTOGRAPHIC RESULTS

It was considered very desirable to correlate the response of the targets with the various explosion phenomena under water such as pulsation, migration, or cavitation. The high-speed motion pictures served this purpose very well. It should be noted, however, that all of these phenomena may have been modified by the presence of a target over the charge and of a bottom only 14 feet below the surface.

Migration

The films show only a blurred picture of the bubble at its collapse. The distance from the target when the bubble collapsed could not be accurately determined directly. Therefore, the position of the bubble at each maximum was measured, and the change of the position between two succeeding bubbles was taken to indicate the total migrations. It was then assumed that the bubble contraction occurred at about half that displacement.

The results of these measurements are shown in Figures 18 through 22. A second set of curves in each of these figures shows the pulse number as a parameter and exhibits the rest position below the surface target. In all cases there was a rest position, so that charges near the target bottom migrated downward, but the rest position was closer to the target than in the case of a free surface without a target. In a few cases a second rest position seems to show up, as is especially apparent for the 8.5-gram tetryl charge below the large block.

Maximum Bubble Radius

The maximum radius of the bubble was measured for those depths at which the bubble showed only a small departure from a spherical shape. For each bubble the diameter was measured in several directions and then averaged. Readings between 40 and 60 inches below the surface were in close agreement. The measured radius for the Hercules Engineer Special cap is 7.25 inches, for the 8-gram pressed tetryl pellets with Number 8 cap 13.4 inches, and for 90 grams PETN plus 5 percent of wax 29.6 inches.

The tetryl and PETN charges produced well-defined images. The radii may be used for calculating the constant  $k_1$  used in the formula for the maximum radius in fresh water

$$R_m = k_1 \frac{\sqrt[3]{W}}{\sqrt[3]{34+d_0}}$$

where  $W$  is the charge weight in pounds,

$d_0$  is the depth of the charge in feet below the surface, and

$R_m$  is the maximum radius of the bubble in feet.

This leads to:

$k_1 = 14.4$  for PETN, and

$k_1 = 14.1$  for pressed tetryl.

The Hercules Engineer Special cap consists, in addition to 0.9 gram of PETN, of a booster charge which contributes to the total energy and is equivalent to 1.24 grams of PETN. It seems, as other experiments show, that

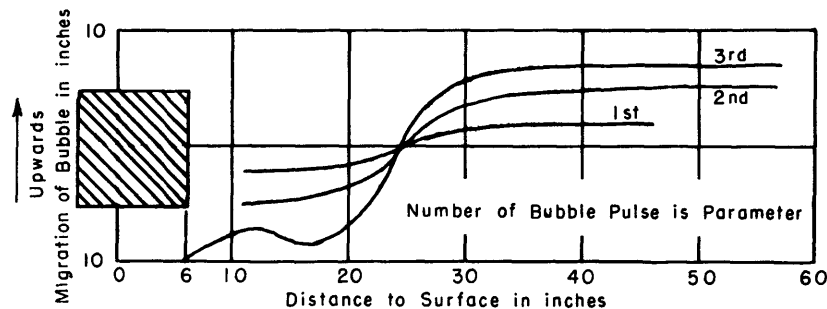
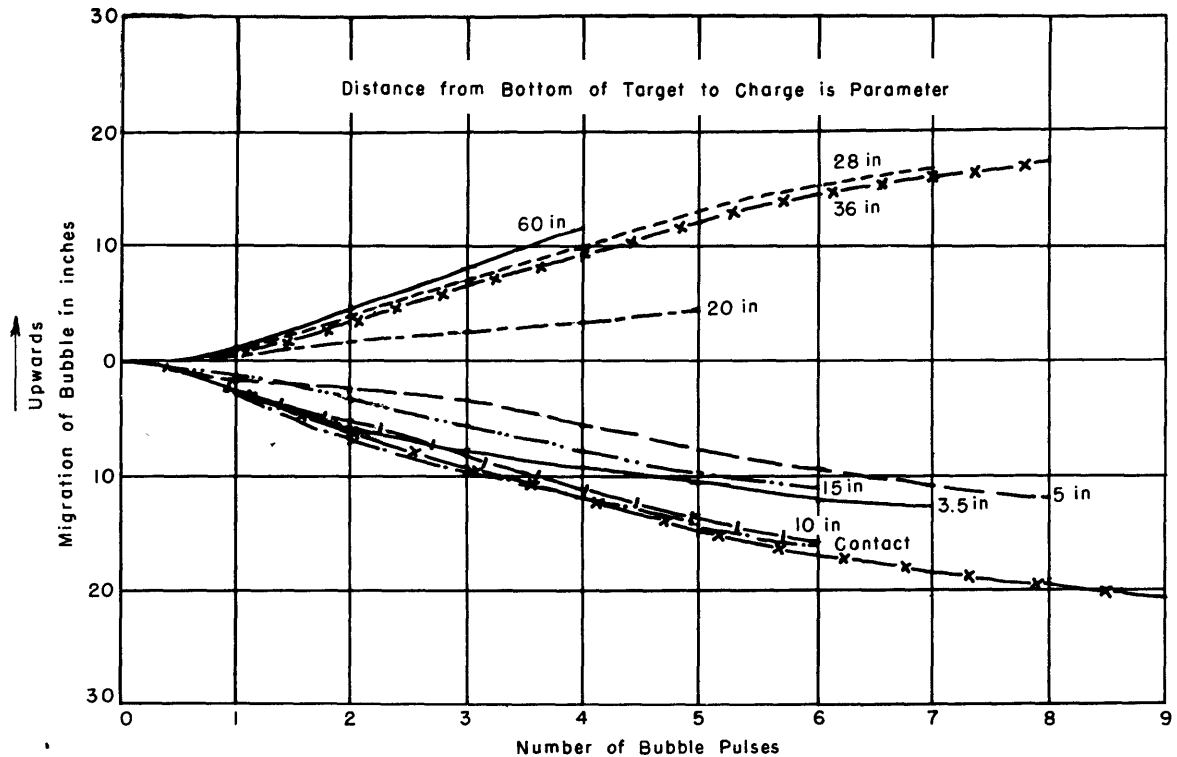


Figure 18 - Migration of Bubble at Various Distances Below Small Block

The charge was a Hercules Engineer Special cap.

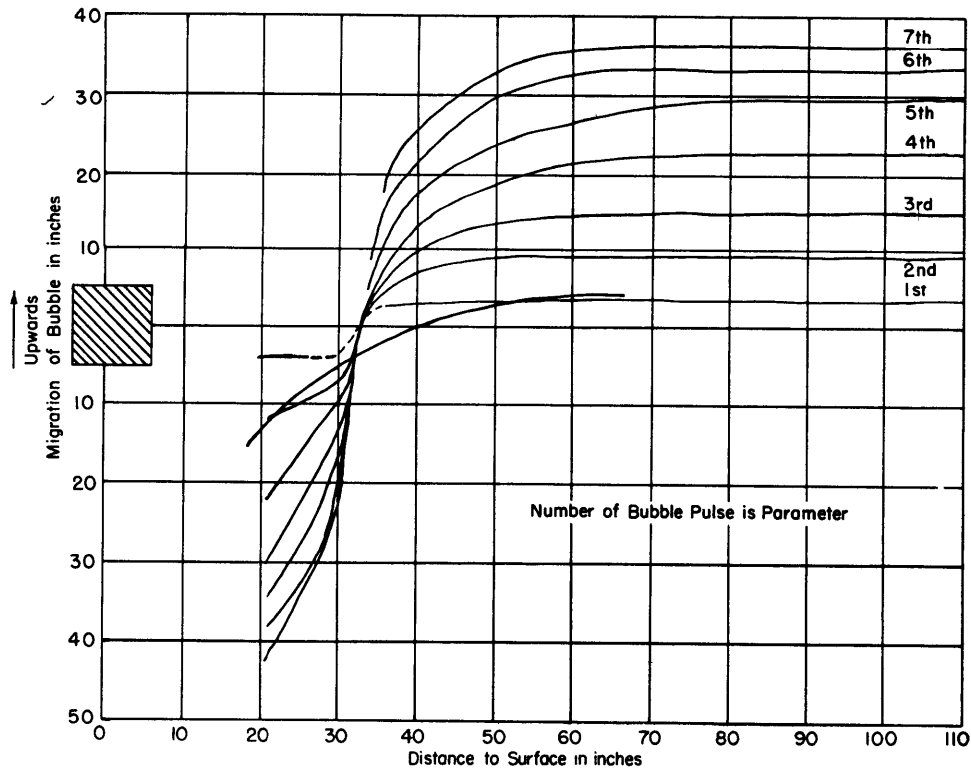
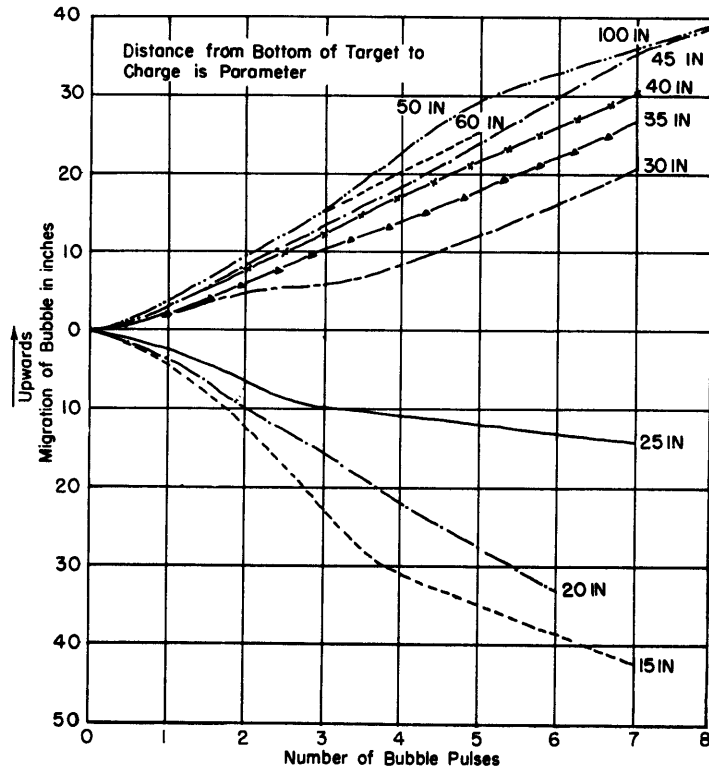


Figure 19 - Migration of Bubble at Various Distances below Small Block

The charge was 8 grams of pressed tetryl with a Number 8 cap.



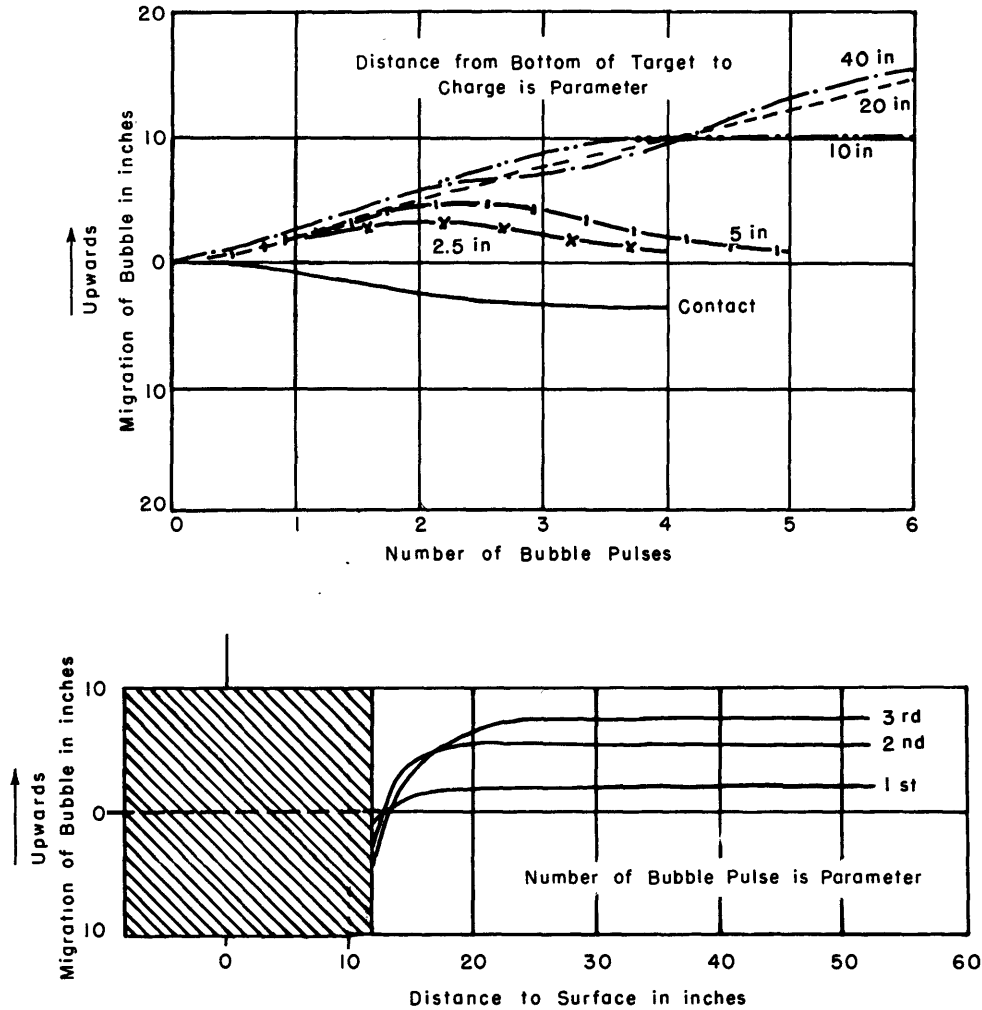


Figure 20 - Migration of Bubble at Various Distances Below Large Block

The charge was a Hercules Engineer Special cap.

the constant  $k_1$  increases for small charges close to the surface, at least for tetryl.<sup>11</sup> Therefore, it might be possible that the value given for the Hercules Engineer Special cap is also somewhat higher than the deep-water value would be.

#### Time Periods of Bubble Pulsation

The time periods  $t_n$  of the bubble pulsations were taken, for the first three pulsations, from the high-speed films as well as from the oscillograph records. No correction was made for either surface or bottom effect. For some tests the time periods could be measured from the response of the target up to the sixteenth bubble pulsation. The differences between the readings

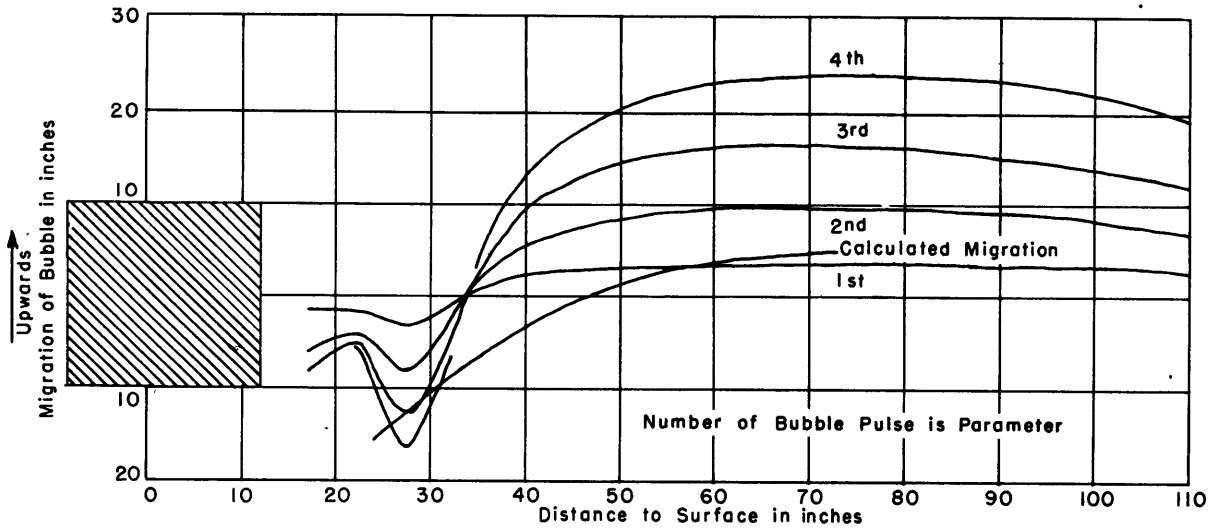
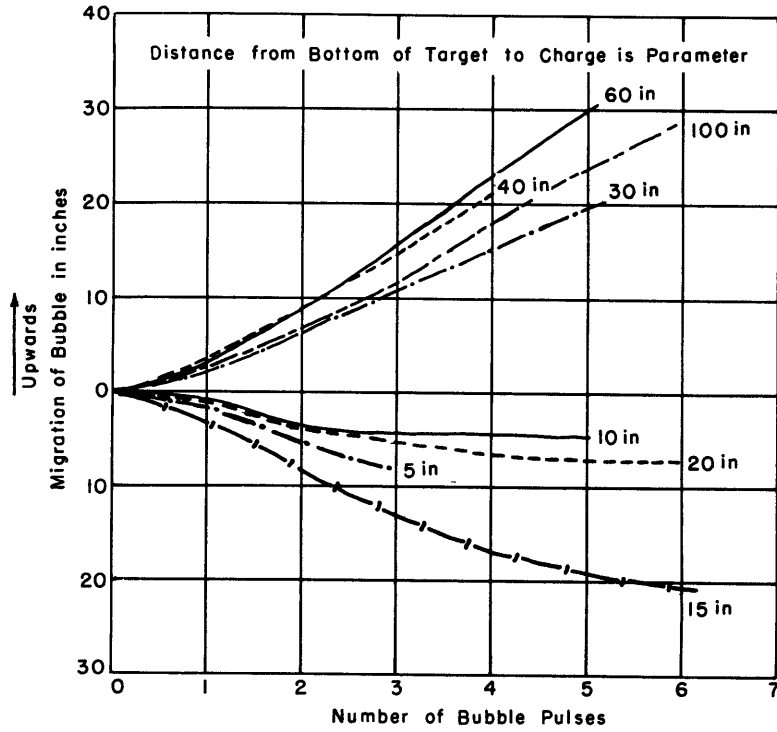


Figure 21 - Migration of Bubble at Various Distances Below Large Block

The charge was 8 grams of pressed tetryl with a Number 8 cap.

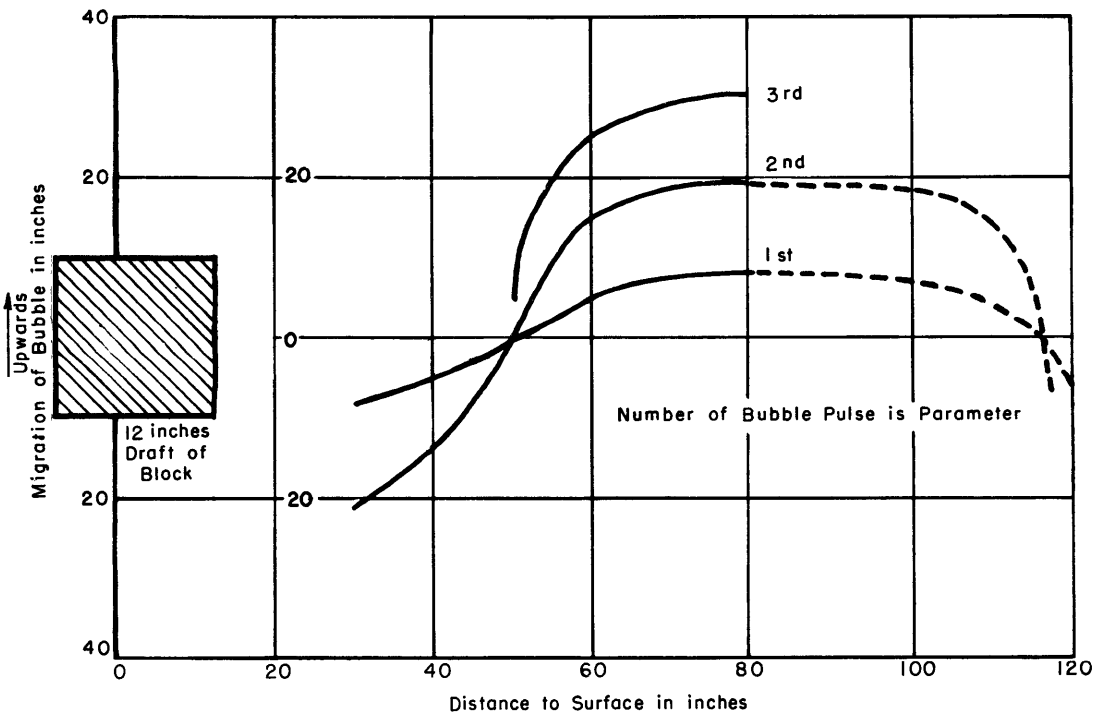
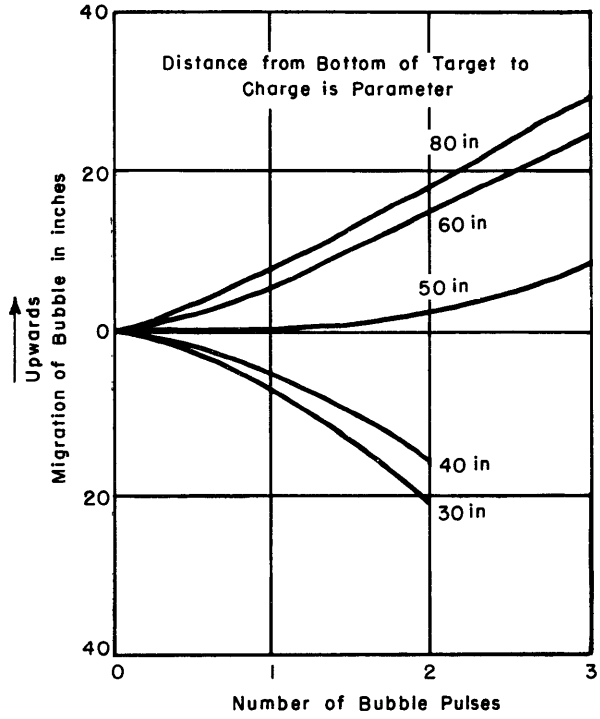


Figure 22 - Migration of Bubble at Various Distances Below Large Block

The charge was 90 grams of PETN plus 5 percent wax.

from the films and from the target responses are small and lie within the errors of the readings. The results are summarized in Table 3.

TABLE 3

Periods of Pulsation of the Gas Globe at Different Initial Charge Depths with Small or Large Blocks at Surface Above the Charge

Initial Charge Depth inches	Time Periods milliseconds								
	$t_1$	$t_2$	$t_3$	$t_4$	$t_5$	$t_6$	$t_7$	$t_8$	$t_9$
Hercules Engineer Special Cap Below Small Block									
42	31.5	23	18.5	18	17.5	16.5	15.7	15	14.5
34	31.5	24	19						
26	30.7	22.5	19						
21	31.5	24.5	20.5						
11	31.9	21	21						
9.5	31.6	22.5	20						
6.5	31.2	20.0	23						
Hercules Engineer Special Cap Below Large Block									
52	31.7	23.8	18	17.5					
32	31.8	24.2	19	17.5					
22	31.2	24	20.5	20					
17	33.9	24	20	18					
12.5	33.9	21.5	19.5	19.5					
8 Grams of Pressed Tetryl and Number 8 Cap Below Small Block									
66	53.8	43	37	35	34				
51	55.4	44	37	36	33	32	29	28	27
41	53.1	44	37	34	34				
36	53.6	43.5	36.5	32	31				
26	55.3	42	37	33	34				
8 Grams of Pressed Tetryl and Number 8 Cap Below Large Block									
72	53.6	44.9	35	35					
42	55.2	44.7	36	35.5	34	32.3	31	29	28
32	54.4	43.4	36	34					
27	55.8	42.7	37	35					
22	54.6	40	36	32					
17	53.0	41.5		32					
90 Grams of Pressed Tetryl Below Large Block									
132	115.8	94.5	70	71					
92	114.5	90	75	71	66	58	54	52	50
72	115.2	93	73	73					
62	113.4	89.5	75	66					
52	112.3	90	72	63					

### Cavitation

The high-speed motion pictures show that cavitation in the very beginning is more pronounced with the small block than with the large block. This cavitation appears in such a short time after the shock wave hits the target that the film speed of 2000 frames per second is not high enough to measure the period between zero time and the appearance of cavitation. Apparently, it is caused by the reflection of the shock wave at the surface and covers only a certain area below the surface. It disappears after a short time, and usually the whole area around the target clears up from the charge position upward to the surface. The phenomena may be complicated, since darker spots and lines show up in the picture. The duration seems to depend on the charge size and is less than 1 millisecond for the Hercules Engineer Special cap and in the order of 2 to 3 milliseconds for the 8-gram tetryl and 90-gram pentolite charges. A clear analysis is difficult because of the irregular shape.

In many cases the first disappearance of the cavitation is followed, after about one millisecond, by another event which seems to involve a large area of cavitation. It extends from close to the bubble, but clearly separated from it, to an area below the target—but not touching it. This phenomenon is not caused by the presence of the target because it may also be seen if the charge is fired below a free surface. So far, no explanation can be given.

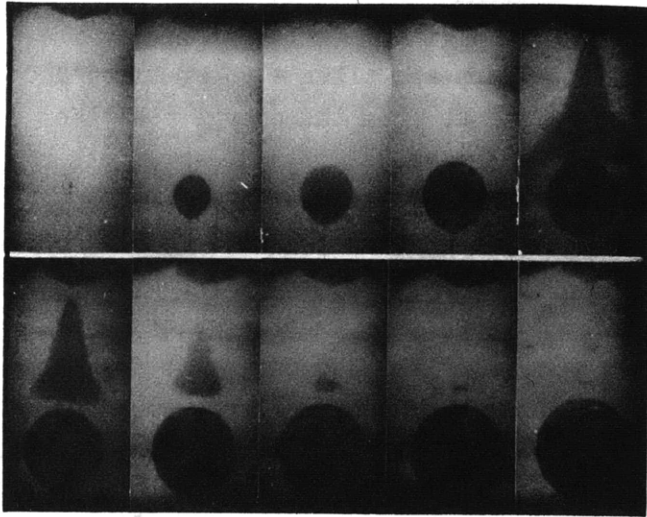
Similar cavitation phenomena can be seen at the first and sometimes at the second bubble pulses. They differ from the initial cavitation in that they disappear not in an upward direction, but downward, at a speed of only a few hundred feet per second. An example selected from one film is shown in Figure 23, together with a velocity record.

### CONCLUSIONS

1. The motion induced in small cube-shaped wood targets when either floating on the surface or submerged was found to be nearly equal to the calculated average motion of the water displaced by the target when the target was not present.

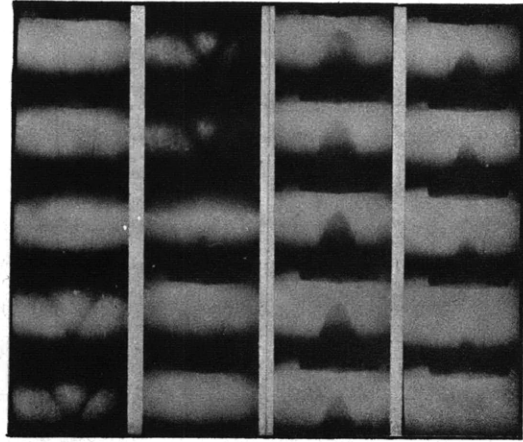
2. The response to the shock wave varies inversely as the distance of the charge from the target, at distances large compared to the dimensions of the target.

3. The target motion corresponds to the incompressive flow of the displaced water during the expansion and contraction of the gas bubble.

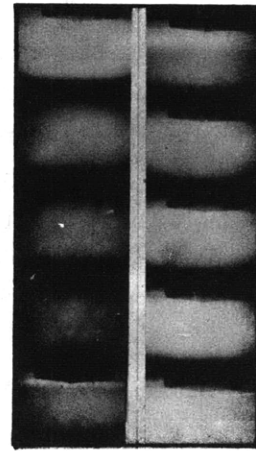


**Initial Stage**

Camera Speed - 900 Frames Per Second



**Initial Stage**



**First Bubble Pulse**

Camera Speed - 2200 Frames Per Second

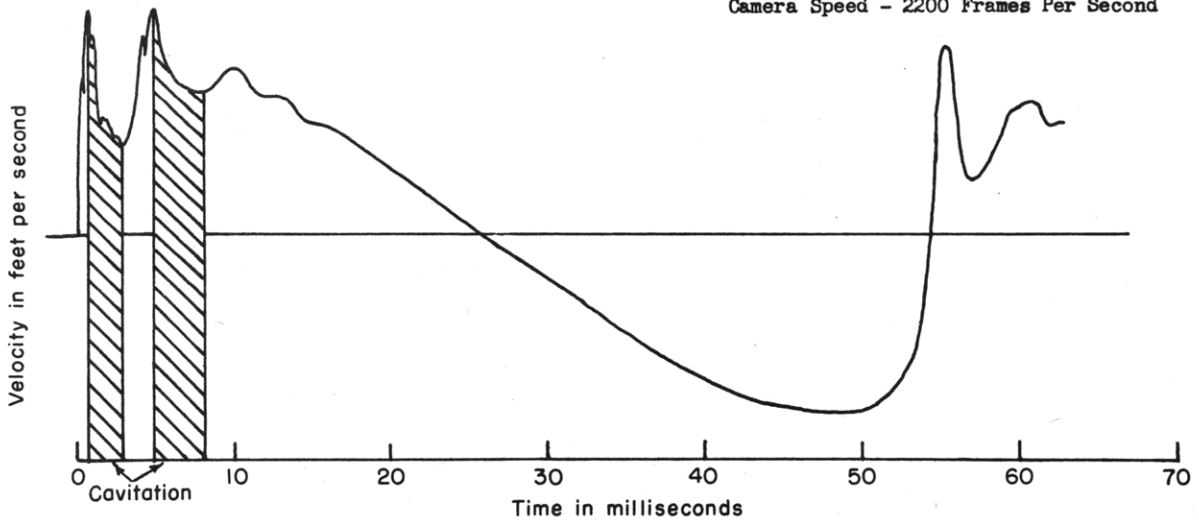


**Figure 23 - Underwater Photographs of Initial Stages after Explosion and Velocity Record**

The charge was 8 grams of tetryl with a Number 8 cap at 40 inches below the large block.

## ACKNOWLEDGMENT

The tests were conducted at the test pond of the David Taylor Model Basin. The initial tests were made by the author, together with Dr. T.A. Perls; the later tests were made with J.G. Batchelder who helped to evaluate the records and who also made the drawings for this report. The underwater high-speed motion pictures were taken by F.B. Kaye and C.H. Johnson. The explosion charges were prepared and fired by C.D. Martin. Mr. W.J. Sette contributed valuable discussions and suggestions. Dr. E.H. Kennard, Chief Scientist of the Structural Mechanics Laboratory, offered many constructive suggestions in reviewing this report.

## REFERENCES

1. Brown, K.S., Comdr., "Effect of Bottom Shape on Target Response, Part A," and Buchmann, E., "Effect of Bottom Shape on Target Response, Part B," Conference on Progress in Research on Ship Protection against Underwater Explosions, UERD CONFIDENTIAL Report 2-50, March 1950.
2. Perls, Thomas A., Ph. D., and Buchmann, Erich, Ph. D., "A Bar Magnet Velocity Meter," TMB Report 723, February 1951.
3. Perls, Thomas A., Ph. D., "A Retraction-Type Displacement Gage," TMB Report 651, March 1950.
4. Perls, Thomas A., Ph. D., and Rich, Harry L., "Evaluation of Selective Shock Instruments," TMB Report 720, to be published.
5. Kennard, E.H., Ph. D., "The Pressure and the Velocity Fields around a TNT Charge Detonated in Free Water," TMB CONFIDENTIAL Report 544, August 1947.
6. Cole, Robert H., "Underwater Explosions," Princeton University Press, Princeton, N.J., 1948.
7. Kennard, E.H., "Report on Underwater Explosions," TMB Report 480, October 1941.
8. Buchmann, E., "Recent Developments in Underwater Explosion Photography at the David Taylor Model Basin," Conference on Progress in Research on Ship Protection against Underwater Explosions, UERD CONFIDENTIAL Report 2-50, March 1950.
9. "Timing Pulse Generator 1000 CPS, Type 61A," TMB Instrumentation Manual, June 1950.

10. Schauer, H.M., "Instruments Employed by the Underwater Explosions Research Division of the Norfolk Naval Shipyard," UERD Report 3-50, July 1950.

11. Swift, E., Jr., and Decius, J.C., "Measurement of Bubble Pulse Phenomena, III. Radius and Period Studies," NAVORD Report 97-46, 11 September 1947.

12. "Sequence Timer, Type 74A, Program Switch for Controlling Detonator and Photo Flash Bulbs," TMB Instrumentation Manual, November 1950.



MIT LIBRARIES DUPL  
3 9080 02754 1058

1912

1

1

1